NORSAR

ROYAL NORWEGIAN COUNCIL FOR SCIENTIFIC AND INDUSTRIAL RESEARCH

Scientific Report No. 2-85/86

SEMIANNUAL TECHNICAL SUMMARY

1 October 1985 – 31 March 1986

L.B. Loughran (ed.)

Kjeller, May 1986

VII.4 NORESS noise spectral studies, preliminary report

A project has been started to investigate NORESS noise recordings on a regular basis, and the objective is to find noise characteristics that are relevant to detection algorithms. The first task has been to determine how the noise varies with respect to frequency, time of day and array geometry. To obtain this an automatic procedure to compute hourly noise spectra for selected beams and single channels has been implemented.

It is important to note in this regard that many model studies earlier conducted on projected seismic monitoring capabilities have been based on estimates of seismic noise levels that have been measured during "quiet" conditions. Even though a standard deviation usually is associated with these levels, it is clear that a much more reliable assessment can be obtained if actual noise measurements over extended time periods are available.

Procedure

The method that has been adopted for the power spectrum estimates is described by T. Kværna and coauthors in the NORSAR Scientific Reports nos. 2-84/85 and 1-85/86. Their method gives smoother spectrum at all frequencies as compared to the direct FFT-spectrum, i.e., we see no large variations in the power estimates at the various frequencies, which is clearly demonstrated in Fig. VII.4.1. The computed beam spectra are based on three different configurations:

Configuration 1 consists of FOZ plus A-ring, plus B-ring, named BRING;
Configuration 2 consists of FOZ plus B-ring, plus C-ring, named CRING;
Configuration 3 consists of FOZ plus C-ring, plus D-ring, named DRING.

The number of instruments are 9 (BRING), 13 (CRING), and 17 (DRING). Beams are formed using infinite velocity, i.e., straight summing of the traces is performed. In addition, we calculate average noise spectrum from the individual Z-component spectra.

The power spectra are computed hourly, using 60 seconds of data, and the procedure runs automatically on the NORESS online computer, (IBM 4341) concurrently with NORESS online recording and RONAPP processing. Care has been taken to avoid any irregularities in the data, and the various checks that are performed are as follows.

A data analysis time window is first selected (starting at the hour). If NORESS has reported any detection within 2 minutes of the hour, the time is adjusted so as to avoid such signals. Various data quality indicators are also inspected, and time is adjusted as necessary to avoid possible bad data segments.

When an acceptable data time interval has been found, RMS is computed for each of the SPZ components. We mask any instrument that has an RMS which differs by more than a predetermined factor from the average RMS for the other Z-components.

Using this procedure we get a set of functions P(f,t,i) where P is the power measured in squared quantum units, f is frequency (512 points), and i is channel number (beam or single sensor; currently 36 total). The variable t is time, sampled each hour, with possible slight adjustments as described above.

Results

Preliminary results from this study are presented in Figs. VII.4.2 through VII.4.7. All of these figures show relative variations in noise power levels (measured in dB), and are based on data uncorrected for instrument response.

Fig. VII.4.2 is a contour plot showing average noise power as a function of time for all NORESS SPZ channels during a typical workday (Monday 7 April 1986). The most significant feature is a sharp increase during day time in the noise power around 6 Hz frequency, and, to a lesser extent, around 12 Hz. These spectral peaks are clearly tied to a localized noise source in the vicinity of the NORESS array (a sawmill located 15 km away), and is repeatedly observed in the data analyzed so far.

Fig. VII.4.3 presented results for the same day as covered by Fig. VII.4.2 as time-domain plots based on a subset of frequencies. We see again that the noise level for frequencies below 2.0 Hz have no significant variations versus the time of day, whereas all higher frequencies are strongly affected by cultural noise. For the 6.0 Hz band we see a 15 dB increase in noise level. However, at the highest frequency shown (16 Hz), the diurnal variations are again relatively modest.

Fig. VII.4.4 and VII.4.5 are similar to Fig. VII.4.3, but cover 1 week of data, respectively.

These figures show clearly the differences in diurnal variations on workdays and holidays, thus confirming that the main source of such variation at frequencies above 2 Hz is cultural activity. An interesting observation is that the noise level at 4 Hz appears to be lower during holidays than at nighttime on workdays, but the significance of this is currently unclear.

These two figures also show that the noise level variation in the 1 Hz band is independent of time of day, but still shows significant fluctuations on more long-term basis. The explanation is that low frequency microseisms generated by, e.g., storm activity in the North Sea have a significant influence at this frequency, but not at frequencies exceeding 2 Hz.

Fig. VII.4.6 shows a comparison between borehole and surface noise power at the NORESS central site. The borehole instrument clearly shows a consistent noise reduction, especially at higher frequencies. However, preliminary investigations have also shown that the P signal level is suppressed in the borehole recordings; thus the actual SNR gain may be quite modest.

Fig. VII.4.7 illustrates the beamforming noise suppression at NORESS using different subgeometries. The data shown correspond to average SPZ noise (MEANZ) and the three geometries BRING, CRING and DRING. The upper figure contains averages within the 3.9 - 4.4 Hz band. In the lower figure there are two parts: The upper part of the figure covering the 0.9 - 1.1 Hz band and the lower part 11.9 - 12.1 Hz. Observations are as follows:

At 1 Hz frequency, the noise is correlated for the innermost part of the array, and only the DRING geometry shows significant noise suppression (about 10 dB).

At 4 Hz, all three geometries show significant noise suppression; in particular the C-ring is effective, averaging almost 15 dB suppresion ($\sqrt{N}$ corresponds to 11 dB). This better than $\sqrt{N}$ suppression is a feature which has been earlier observed, and is tied to extracting "optimum" subgeometries for given frequencies, thus taking advantage of "destructive" noise correlation.

At 12 Hz, the noise is uncorrelated, and the three geometries give each approximately $\sqrt{N}$ noise suppression.

In summary, these preliminary investigations have already provided important insight into the noise characteristics observed at NORESS. While many of the features (e.g., the strong 6 Hz peak) are clearly tied to the actual local conditions particular to the NORESS site, other characteristics (such as the better than $\sqrt{N}$ beam noise reduction in some cases) could well have more general application. We plan in future studies to compile more comprehensive statistics in order to fully evaluate the noise characteristics at NORESS, and will in particular study the correlation between noise level and local wind conditions. We will also incorporate noise spectra from the NORESS High Frequency Seismic Element in order to expand the studies to include higher frequencies.

J. Fyen

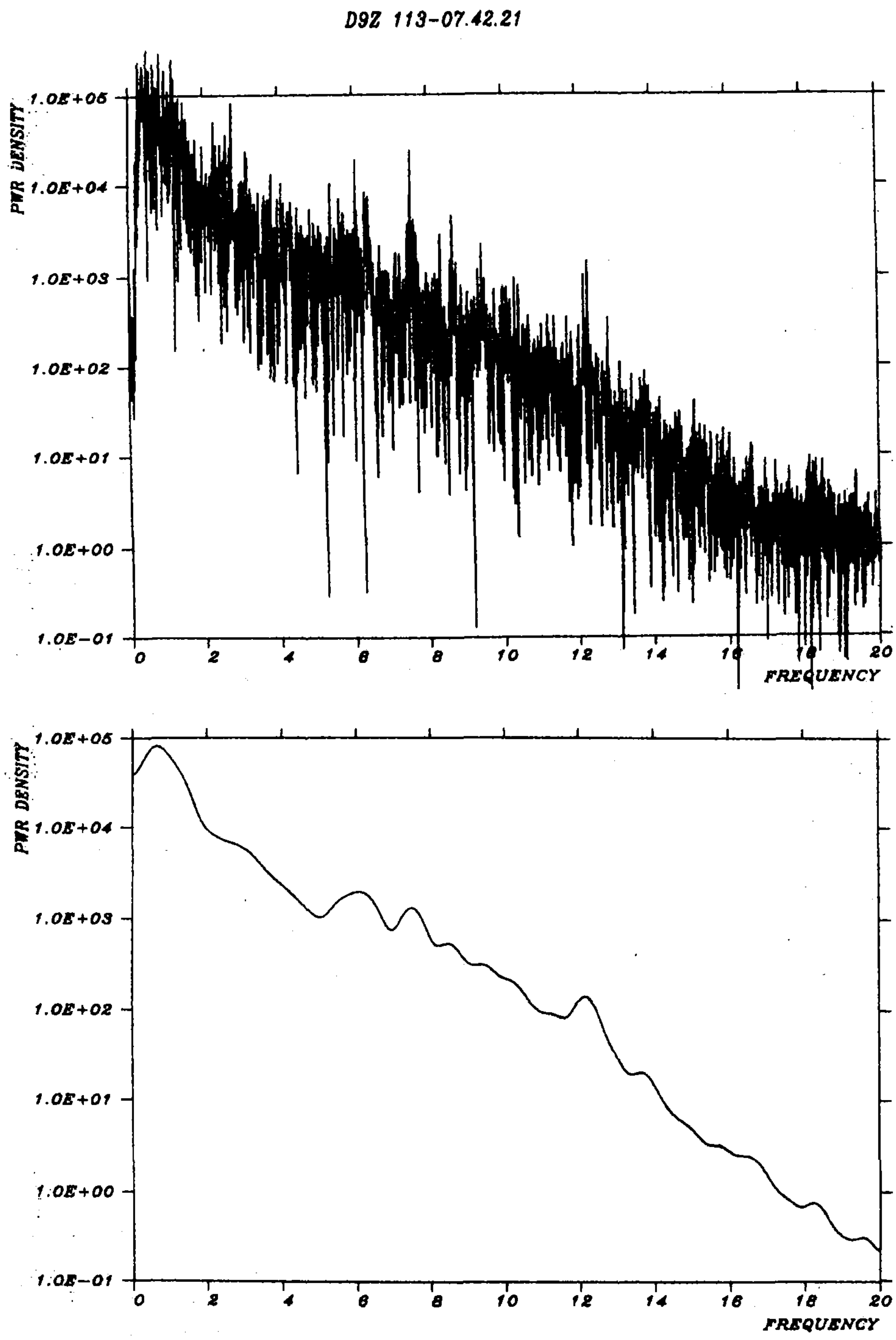

Fig. VII.4.1 The upper figure shows power spectrum for D9Z, using 60 sec of data and direct FFT. The lower spectrum is obtained by a prewhitening of the data, windowing the autocorrelation and then transforming this function. The resulting spectrum is then compensated for the pre-whitening and is shown to be very smooth.

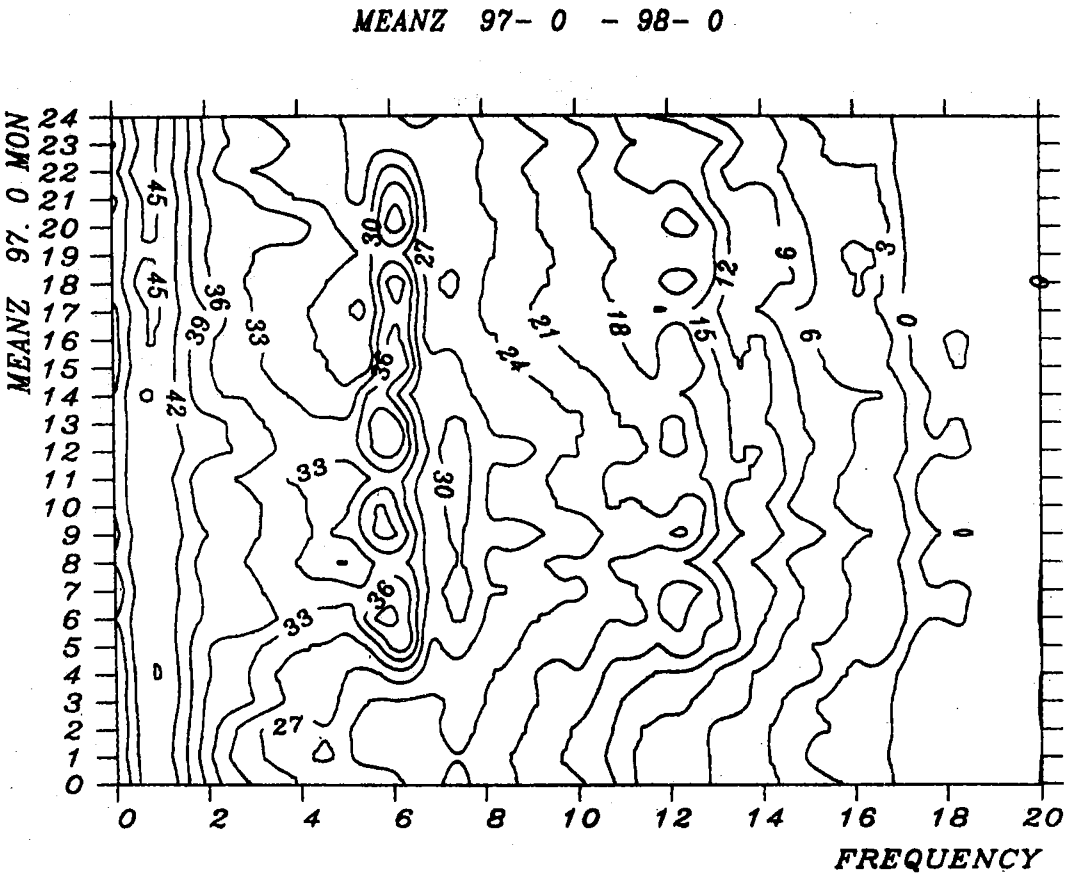

Fig. VII.4.2 This figure shows average power for all NORESS SPZ channels plotted versus time (00-24) and frequency. There are 25 points (hours) in time axis, and 512 points in frequency. We can see a clear peak in the power distribution starting at time 0400 GMT and frequency 6.0 Hz. This peak is due to activities in a saw-mill located approximately 15 km from the array. It is seen that the noise power increases during day time, to a lesser extent, also at other frequencies, except in the lowest frequency band (below 2 Hz).

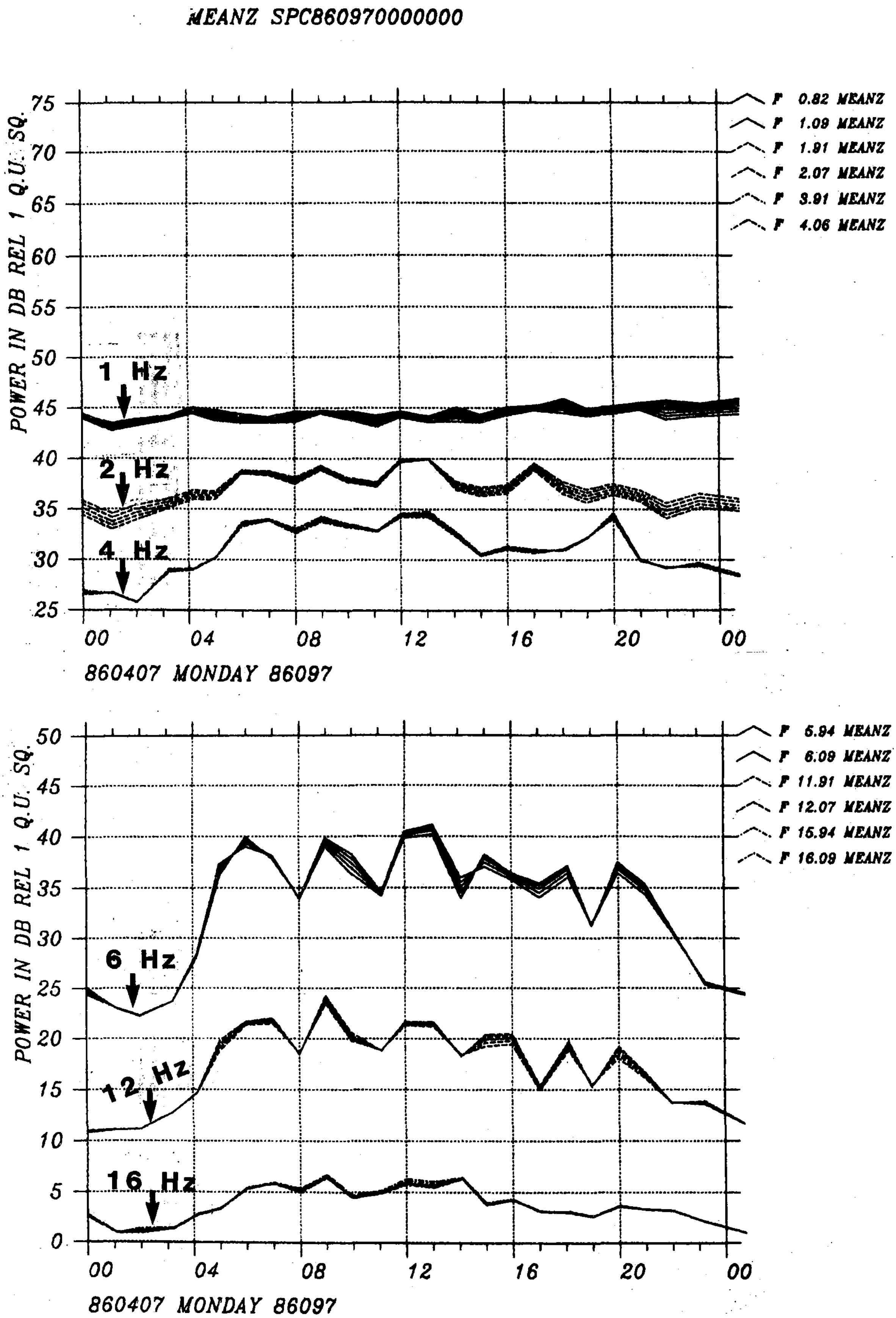

Fig. VII.4.3 Average NORESS SPZ spectral levels as a function of time of day for a typical workday (Monday, 7 April 1986). The plot shows a sequence of narrow bands (±0.1 Hz) around the indicated frequencies. Note the relative stability of the spectral levels except at 6 and 12 Hz, as explained in the text.

MEANZ SPC861040009030

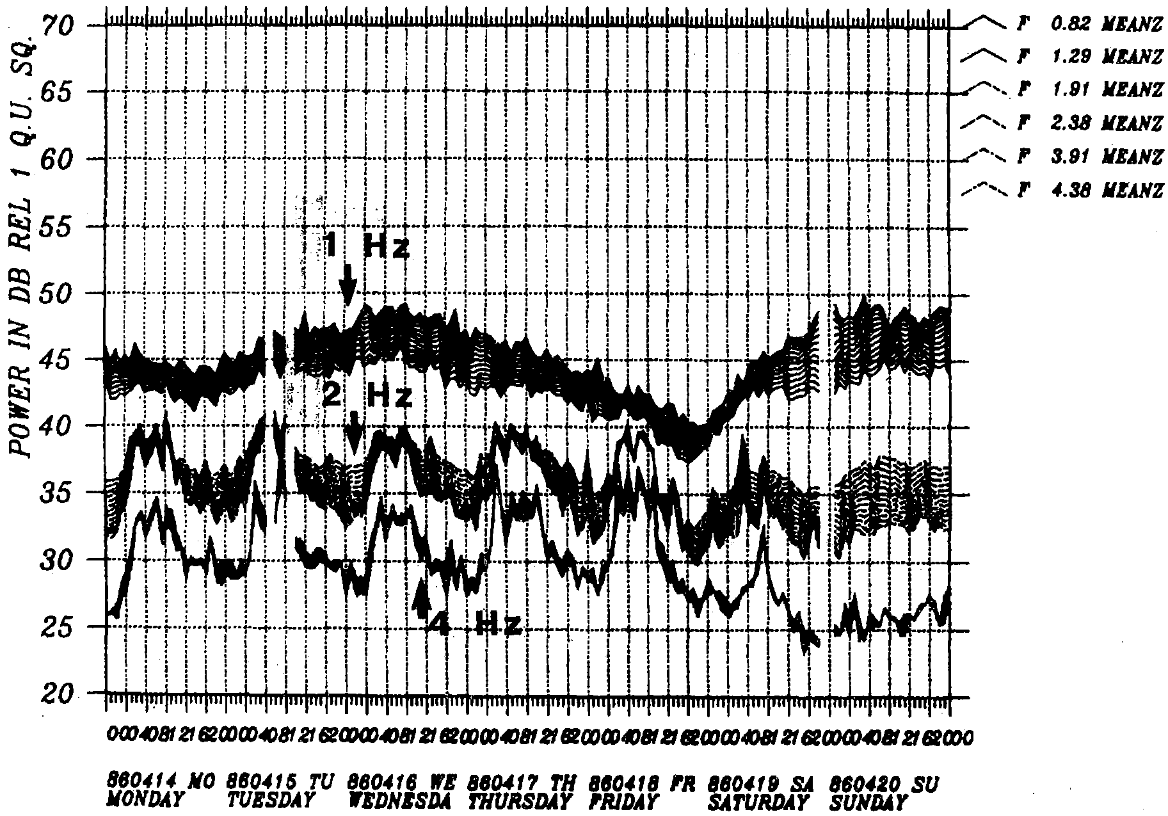

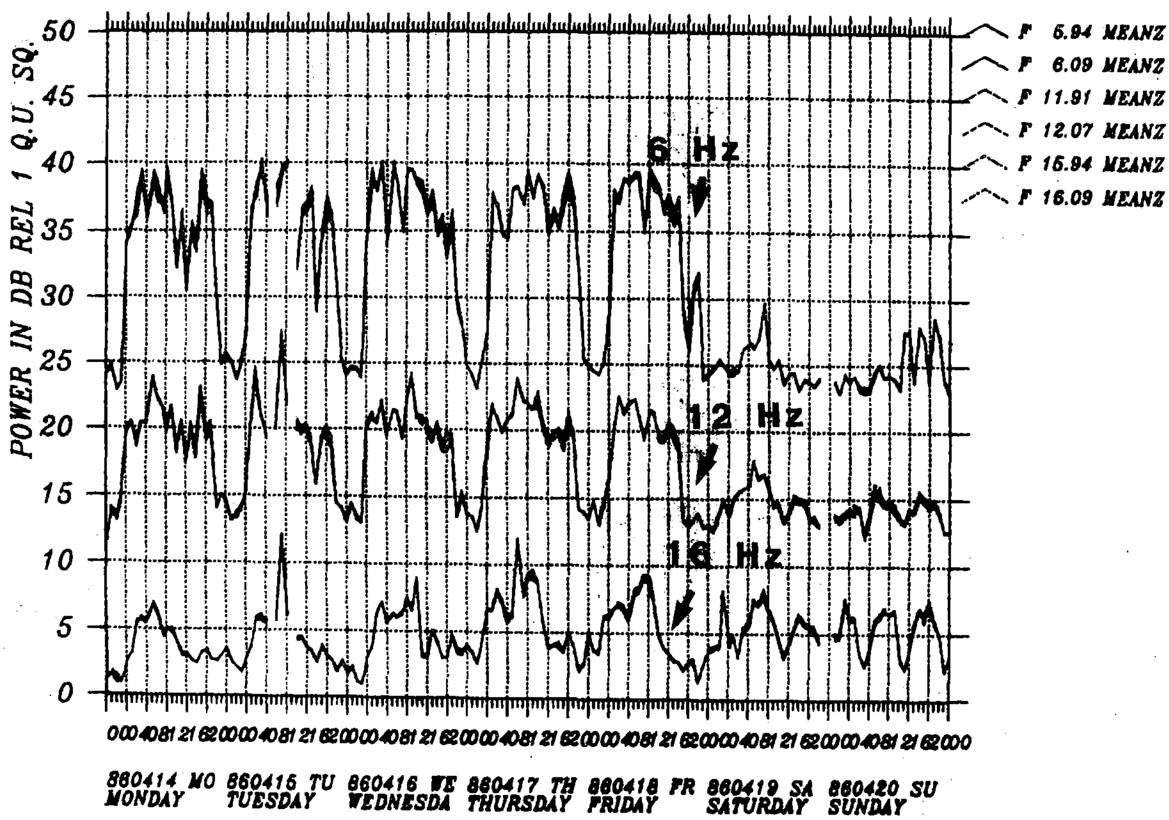

Fig. VII.4.4 Average NORESS SPZ spectral levels for the week Monday 14 April through Sunday 20 April 1986 (cf. Fig. VII.4.3). Note the lack of diurnal variations during the weekend. Also note the slow variations in the band around 1 Hz. This is due to low frequency microseisms, and is not seen at higher frequencies.

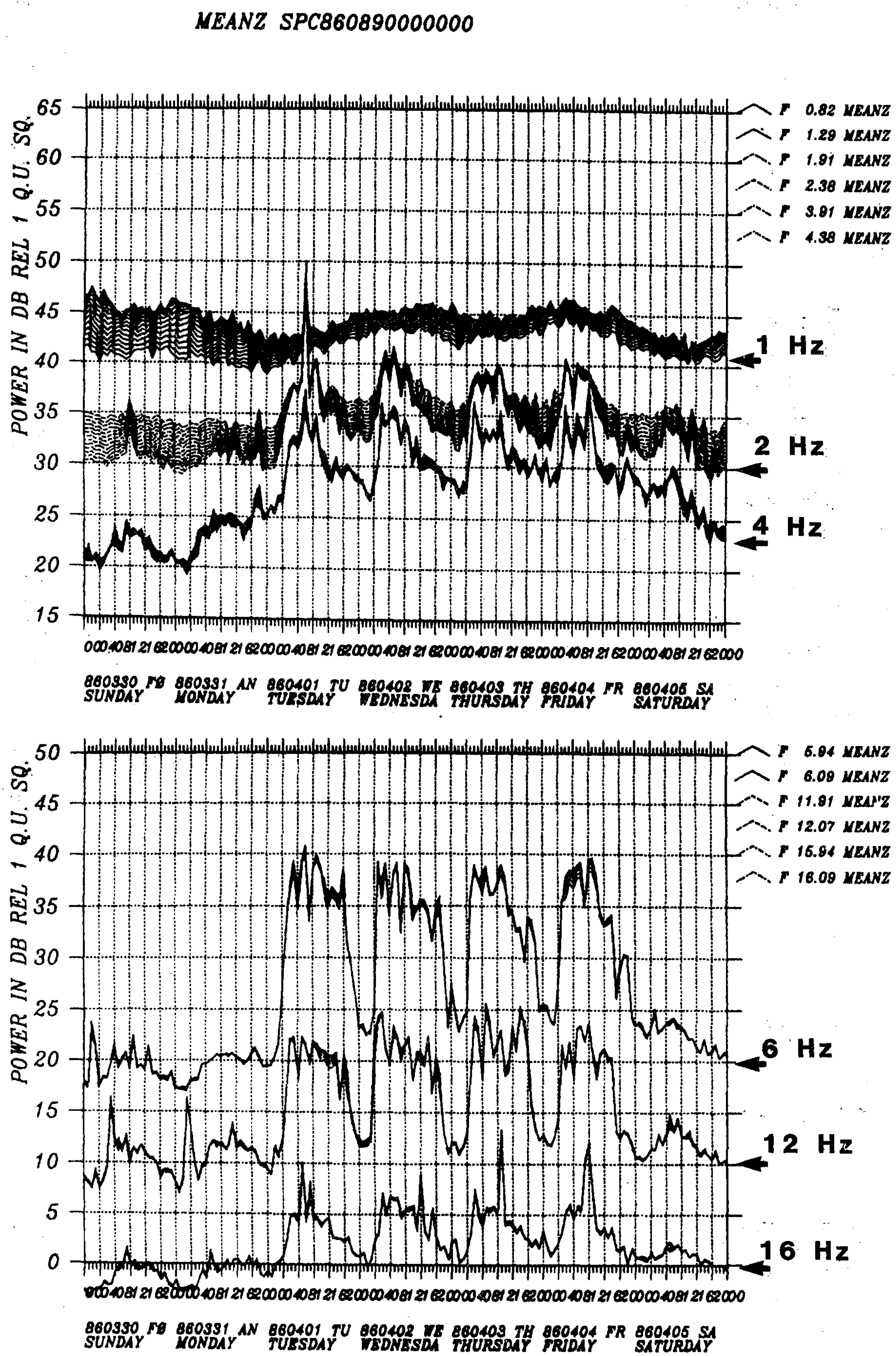

Fig. VII.4.5 Same as Fig. VII.4.4, but for the week starting Sunday, Easter day. Note that Sunday, Monday and Saturday of this week are holidays. See the comments for Fig. VII.4.4.

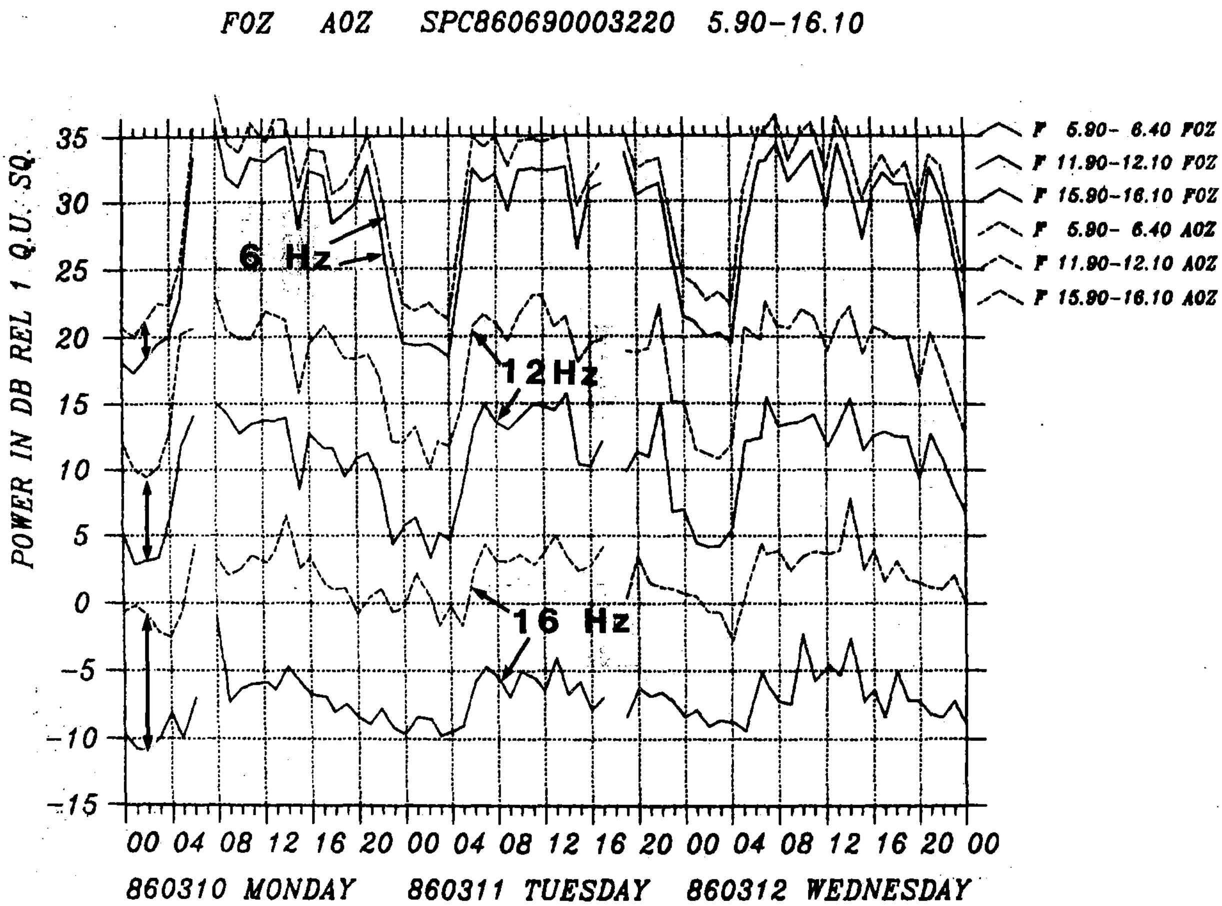

Fig. VII.4.6 Three-day comparison of surface noise level (AOZ, stippled lines) and borehole noise level (FOZ, solid lines) at three frequencies. Note the larger borehole noise suppression at higher frequencies.

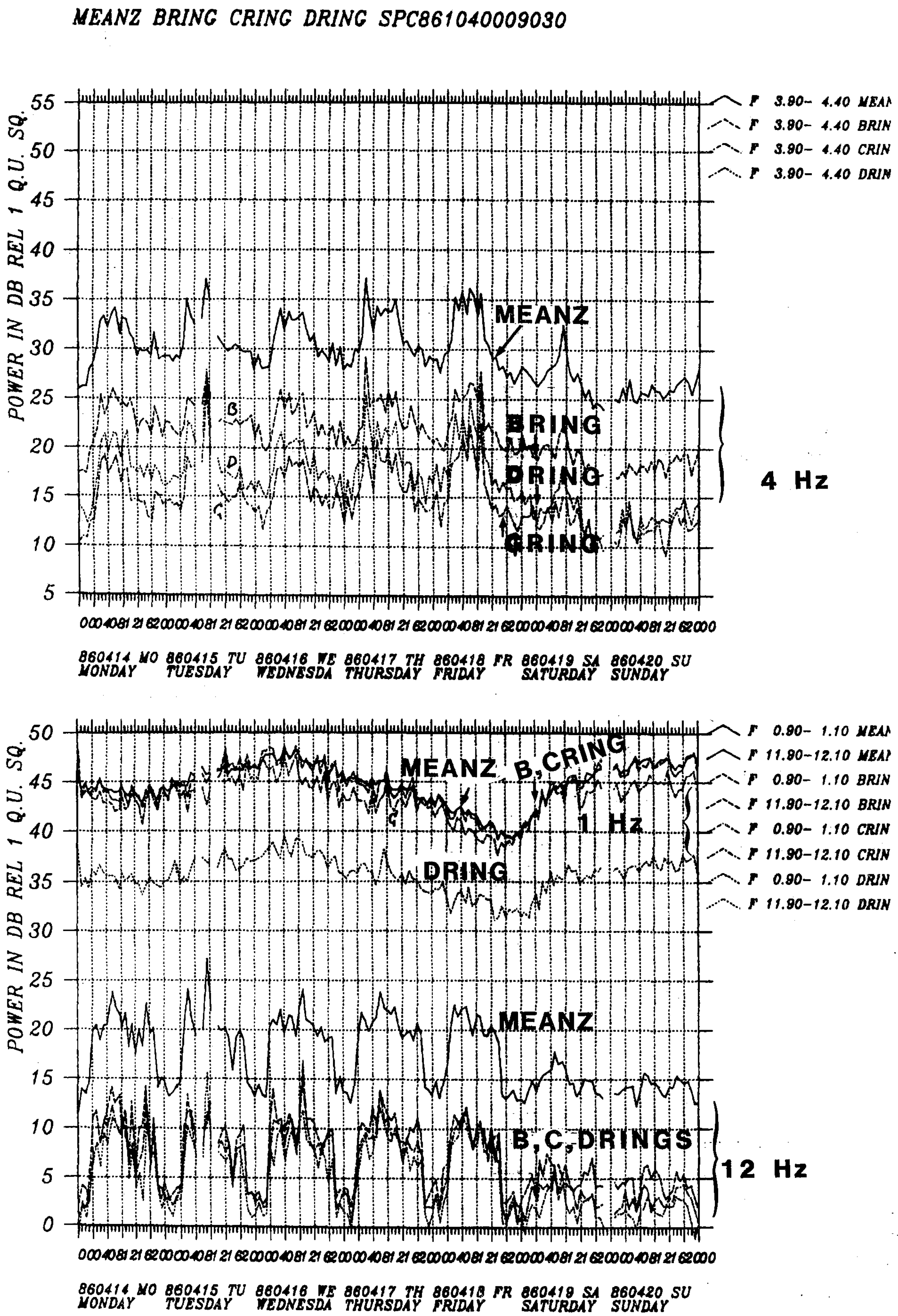

Fig. VII.4.7 Comparison of average SPZ noise with beam noise for three beam configurations (see text). Note that at 1 Hz only the D-ring provides significant noise suppression. At 4 Hz, the C and D rings are most effective. At 12 Hz, the three beams are similar.